BNL-65383

GEOPHYSICAL RESEARCH LETTERS, VOL. 25, NO. 4, PAGES 513-516, FEBRUARY 15, 1998

Apportionment of light scattering and hygroscopic growth to aerosol composition

Lynn McInnes, Mike Bergin* and John Ogren

NOAA Climate Monitoring and Diagnostics Laboratory, Boulder, CO

Stephen Schwartz*

*Brookhaven National Laboratory, Environmental Chemistry Division, Upton, NY

Abstract. During a recent campaign at the NOAA CMDL monitoring station on Sable Island, Canada (43.93° N, 60.01° W) a dual-nephelometer humidigraph measured the hygroscopic growth factor of aerosol scattering, $f_{RH}(\sigma_{sp})$, one of the key parameters necessary for estimating short-wave aerosol radiative forcing. Measurements revealed less growth for anthropogenically influenced aerosols than for marine, $f_{RH}(\sigma_{sp})$ of 1.7 ± 0.1 vs. 2.7 ± 0.4, where $f_{RH}(\sigma_{sp}) = \sigma_{sp(85\%)}/\sigma_{sp(40\%)}$. A combined measurement-modeling approach was used to estimate σ_{sp} and its RH-dependence, based on the measured particle size distribution and composition. The model suggested that differences in the particle size distribution, assuming the same aerosol composition, could not explain the observed differences in $f_{RH}(\sigma_{sp})$. We have confirmed with individual particle analysis, that aerosol composition was indeed responsible for the difference in $f_{RH}(\sigma_{sp})$. As well, the scattering contribution of organic carbon for the influenced case is at least as much as sulfate aerosol.

Introduction

Tropospheric aerosols influence the earth's radiation balance by scattering and absorbing a portion of the incoming short-wave solar radiation, and by modifying the optical properties of clouds, including their spatial extent and lifetime. In contrast to well-mixed greenhouse gases, the aerosol spatial distribution is highly non-uniform with respect to aerosol mass and particle size distribution, confined to roughly the lowest 2 km, dependent on proximity of aerosol source regions, aerosol lifetimes which are size dependent, and the ability of particles to activate in cloud. The magnitude of direct radiative forcing estimates depends on several parameters including mass scattering efficiency, relative humidity dependence of aerosol scattering, and aerosol mass loading [*Schwartz, 1996*]. Calculations of global energy balance suggest that the net effect of tropospheric sulfate aerosol on regional climate is a negative forcing (net cooling), with significant cooling expected over industrial regions of the Northern hemisphere [*Charlson et al., 1992*].

Dry salt particles when exposed to sufficient concentrations of water vapor will rapidly deliquesce, i.e. transform into solution droplets. The RH of deliquescence is dependent on the water-solubility of the salt, i.e. is composition dependent. Ambient measurements of hygroscopic growth of aerosols from Seattle, WA and Denver, CO attributed the lack of a discernible deliquescence point to a mixed and variable aerosol composition [*Covert et al., 1972*]. Rood and co-authors [*1985*], with similar observations in Riverside, CA noted that the aerosol deliquescence returned after heating to 200° C, suggesting internal mixtures of hygroscopic and non-hygroscopic material. Both hygroscopic and non-hygroscopic modes were observed for aerosol in Los Angeles the Po Valley, with diameter factor, $f_{RH}(D_p) = D_{p(90\%)}/D_{p(20\%)} = 1.0$ (no growth) to 1.5 [*McMurry and Stolzenberg, 1989; Svenningsson et al., 1992*].

Airborne measurements of hygroscopic growth of aerosol scattering over the CA and WA coast revealed values of $f_{RH}(\sigma_{sp}) = \sigma_{sp(80\%)}/\sigma_{sp(30\%)}$ between 1.2 and 3.3, with little or no altitude dependence [*Hegg et al., 1996*]. The authors attributed the variability to differences in the mass median diameter of the aerosol, with an inverse dependence on size. Values of $f_{RH}(\sigma_{sp})$ are somewhat dependent on the lower RH valve selected for the comparison, and are commonly (although not always) taken in the range 20 to 40% RH.

In September of 1996, we conducted a 2-week field campaign at Sable Island. Our primary motivations were to obtain measurements of $f_{RH}(\sigma_{sp})$ for marine, continental, and anthropogenically influenced airmasses selected on the basis of isentropic airmass trajectory analyses [*Harris and Kahl, 1994*], and to examine its dependence on the measured particle size distribution and composition. Because the relative contribution of organic aerosols to the light scattering budget and their influence on hygroscopic growth are relatively unknown, we used size dependent composition measurements to apportion scattering to sea salt, sulfate, organic, and mineral aerosol. We modeled the aerosol scattering coefficient (σ_{sp}) based on measurements of the dry particle size distribution and size-dependent composition and compared results with in-situ measurements of σ_{sp} as a function of RH.

Aerosol Measurements

The NOAA CMDL aerosol program consists of a network of Northern hemisphere monitoring stations designed to characterize the means, variabilities, and trends of climate forcing properties for different aerosol sources [*Ogren et al., 1996*]. Climatically-relevant aerosol parameters at Sable Island, Canada (43.93° N, 60.01° W) have been monitored continuously since August 1992 as a joint collaboration with the Atmospheric Environment Service of Environment Canada. The absence of local emission sources and proximity to the North American continent makes Sable Island well suited for monitoring anthropogenic aerosol advected from the northeastern US, and marine aerosol from the Northern Atlantic.

Copyright 1998 by the American Geophysical Union.

Paper number 98GL00127.
0094-8534/98/98GL-00127$05.00

Aerosol measurements at Sable Island routinely include number concentration, light scattering and absorption, mass concentration, and water-soluble ionic composition, measured for the sub 10 and 1 μm aerosol. Air drawn into the sampling stack at a flow rate of 1 m^3 min^{-1} spends ~7 seconds in the stack before entering a heated inlet section designed to maintain the RH of the airstream at 40%. The humid marine environment of Sable Island in the summertime can require as much as 16° C heating to achieve the desired RH. Evaporative losses are small, corresponding to at most a 20% decrease in the aerosol scattering for volatile compounds such as ammonium nitrate [*Bergin et al., 1997*]. A flow splitter divides the airstream into 5 separate pathways; one line delivers aerosol to the nephelometer at 30 slpm, one to an automated filter carousel at 30 slpm, and the remaining lines are connected to vacuum to maintain a total flowrate of 150 slpm. Large particles are removed by 10 μm impactors preceding the nephelometer and filter carousel. The aerosol pathway is automatically switched between impactors (10, 1 μm) in front of the nephelometer to evaluate the relative scattering contribution. The control RH ensures that the same nominal size-cut is used, and eliminates the confounding influence of ambient RH and T on the measurements.

A TSI 3563 Integrating Nephelometer (ThermoSystems Inc.) measured the total light scattering of airborne particles at three visible wavelengths (450, 550 and 700 nm). The hygroscopic growth parameter of aerosol scattering, $f_{RH}(\sigma_{sp})$, is a relative measure of the aerosol scattering coefficient at high and low RH, represented as $\sigma_{sp(RH>40\%)}/\sigma_{sp(40\%)}$, where 40% RH is the sampling control. Such quantities are directly measurable with a dual-nephelometer humidigraph [*Koloutsau-Vakakis et al., 1994*]. One nephelometer continuously measures the aerosol scattering coefficient at the control RH, while the second measures σ_{sp} between 50 and 90% RH, alternating sub 10 μm and sub 1 μm aerosol at the control humidity every 30 minutes. A RH, T sensor records airstream conditions in the nephelometers .

The particle number size distribution from 0.02 to 0.50 μm diameter was measured with a Scanning Mobility Particle Sizer (SMPS, TSI 3934). Diffusion dryers maintained the airstream humidities below 20% RH, with RH, T sensors recording conditions. Flowrate drift was eliminated with mass flow controllers. The particle number concentration ($D_p > 0.015$ μm) was monitored with a condensation nucleus counter (TSI 3760). Integrated number concentrations from the SMPS system agreed within 10% of the CN establishing that most of the particles were in this size range.

Aerosols were collected for individual particle analysis twice daily (2-10 minute collection) using a multistage low pressure cascade impactor. The particle size distribution and composition (using x ray analysis) was determined with electron microscopy (EM) techniques [*McInnes et al., 1997*] for particles $0.06 \leq D_p \leq 2.0$ μm, assembled from low magnification digital images of the deposit. The projected area of each particle in 2-D was converted to an aerosol diameter based on appropriate conversion factors for laboratory particles of known size. Agreement was obtained with respect to the relative number of particles in each bin of the SMPS and EM size distributions, to within ±20% of the number.

Table 1. Sector Designator for Marine and Influenced Case.

Day, 1996	wind sector	σ_{sp}_G (sub 10 μm)	fraction sub 1 μm
265	2, 3, 0	15.1 ± 2.6	0.37 ± 0.03
268	3, 1, 0	4.5 ± 1.2	0.15 ± 0.02

Sector code = 0 indicates the trajectory remained in the previous sectors.

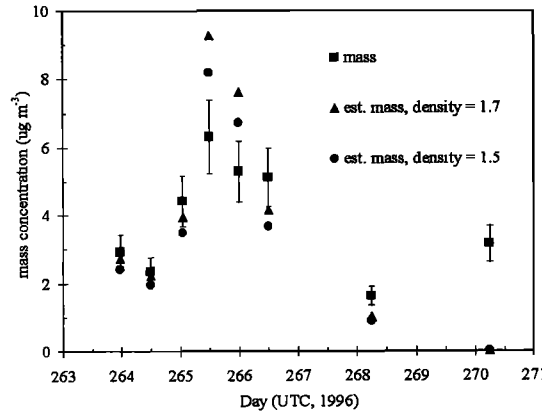

Figure 1. Aerosol mass concentration from gravimetric analysis of filters and estimates from the particle size distribution. Error bars indicate the uncertainty in the gravimetric analysis.

A second impactor collected particles between 1 and 10 μm for subsequent analysis. Downstream, 12 hour filter samples were collected with an automated carousel system, which were subsequently weighed in a controlled atmosphere at 30 ± 2% RH (20° C) at NOAA PMEL. After weighing, the filters were extracted and analyzed for water soluble anions (SO_4^{2-}, Cl^-, NO_3^-, Br^-) and cations (Mg^{+2}, NH_4^+, Ca^{2+}, Na^+, K^+) using ion chromatography. Differences between the gravimetric and total ionic mass indicate the presence of additional aerosol components, such as carbonaceous or insoluble mineral aerosol.

Modeling f_{RH} of Aerosol Scattering

The aerosol scattering coefficient, $\sigma_{sp(40\%)}$, for the sub 1 μm aerosol was estimated for each case as:

$$\sigma_{sp(40\%)} = \frac{\pi}{4}\sum_{j=1}^{m} D_{pj}^2 K(\lambda)_{Sj}\ n_{Tj}$$

where the particle size distribution was represented as 20 separate size bins (m = 20) between 0.01 and 1.0 μm diameter where n_{Tj} is the number of particles counted in each bin of mean diameter, D_{pj}. The approximation of Bohren and Huffman [*1983*] was used to represent the Mie scattering efficiency of spherical particles, $K(\lambda)_{sj}$, wavelength λ = 550 nm assuming a refractive index of 1.5 - 0i. Uncertainty in the refractive index of ±10% (1.35 to 1.65) results in only a 20% uncertainty in the estimated aerosol scattering coefficient. For high RH conditions, the aerosol scattering coefficient, $\sigma_{sp(RH)}$, was modeled as:

$$\sigma_{sp(RH)} = \frac{\pi}{4}\sum_{j=1}^{m} D_{pj}^2 f_{RH}(D_p)^2\ K(\lambda)_{Sj}\, n_{Tj}$$

where $f_{RH}(D_p)$ is the diameter growth factor. The equations can be used to estimate the increase in aerosol light scattering, $f_{RH}(\sigma_{sp})$, for various diameter growth factors.

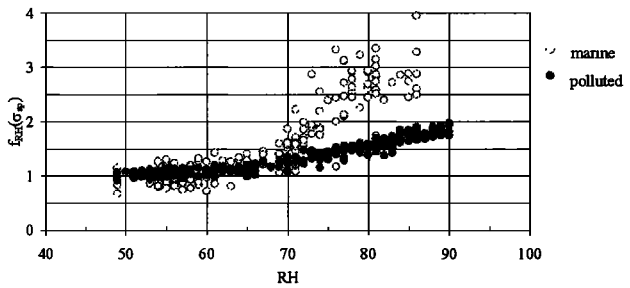

Figure 2. Hygroscopic growth factor of aerosol scattering, $f_{RH}(\sigma_{sp})$, measured for the marine and anthropogenically influenced case. The greater scatter for the marine case is caused by much lower aerosol concentrations.

Results and Conclusions

Airmass trajectories for the two cases are summarized in Table 1 as a three character code indicating the order of passage into different wind sectors where 1 = marine (0° to 225°, where 0° = N), 2 = anthropogenically influenced (225° to 305°), and 3 = clean continental (305° to 360°) [*Harris and Kahl, 1994*]. The marine period (268 to 269) had trajectories originating over the open ocean in the lowest 500 m of the marine boundary layer, crossing into the clean continental sector before arrival at Sable Island. For this period, CN and σ_{sp} were low (< 500 cm^{-3}, and < 5 Mm^{-1} at 40% RH). The submicrometer fraction of the total scatter was 0.15, suggesting that most of the scattering was from coarse sea salt aerosol. This is consistent with findings by Hoppel et al. [*1990*] of a large role for sea salt aerosol in the light-scattering budget of the marine boundary layer.

Relatively stable meteorological conditions were encountered on days 264.5 to 267.5, coincident with transport of anthropogenically influenced air from the northeastern US. CN concentrations were > 1000 cm^{-3} and σ_{sp} (sub 1 μm) was 10 to 20 Mm^{-1} (40% RH), representing at times 60% of the total scatter. Mass concentrations were 3 to 5 times higher than marine conditions.

Mass concentrations (sub 1 μm) are shown in Fig. 1 for filters with > 15 m^3 of air volume. The aerosol mass as estimated from the particle size distribution (ρ = 1.7 or 1.5 g cm^{-3}) is also shown. We present a case study of days 265 and 268,

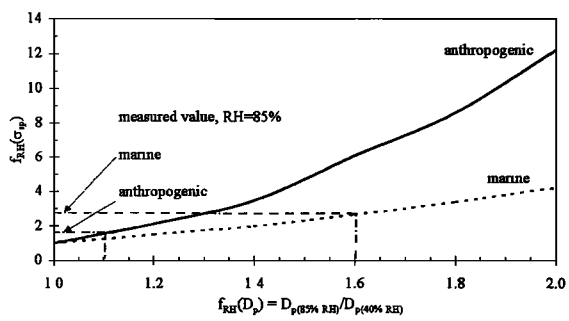

Figure 3. The hygroscopic growth factor of aerosol scattering, $f_{RH}(\sigma_{sp})$ estimated for many values of the diameter growth factor, $f_{RH}(D_p)$, using measured particle size distributions for both cases. Measured values of $f_{RH}(\sigma_{sp})$ from the humidigraph nephelometer at 85% RH are indicated suggesting a diameter growth factor of 1.6 for marine aerosol, and significantly less growth for the anthropogenic aerosol in which $f_{RH}(D_p)$ = 1.1.

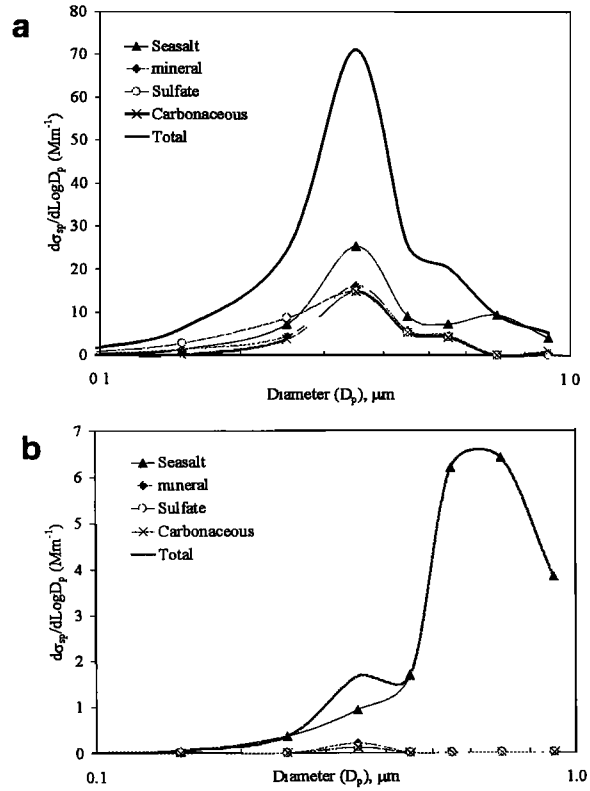

Figure 4. Relative scattering contribution of different aerosol types for a) anthropogenically influenced and b) marine case. Most of the submicrometer scattering is due to sea salt aerosol in the marine case.

representing anthropogenically influenced and marine airmasses, respectively. The periods were selected because of an obvious difference in hygroscopic growth, $f_{RH}(\sigma_{sp})$, shown in Fig. 2. For the marine case the aerosol was quite hygroscopic, exhibiting an almost 3 fold increase in $\sigma_{sp(85\%)}$, similar to natural sea salt aerosol [*Pueschel et al., 1969*]. The growth of σ_{sp} for the anthropogenic case was noticeably lower at 1.7 ± 0.1.

Three aerosol modes were observed for the marine number size distribution with diameters 0.037, 0.146, and 0.55 μm. For the anthropogenically influenced case a dominant mode was observed at 0.087 μm, with significant tailing at larger sizes, which may indicate an external mixture of aerosol types. A second mode was observed at 0.55 μm. The small concentrations of smaller particles suggests the aerosol is aged.

The light scattering coefficient at the control RH was modeled for each case from the particle size distributions. Modeled and measured values of σ_{sp} for the anthropogenic case agreed to within ±20%. For the marine case, the model underestimated the aerosol scattering by 40%. This underestimation may be due in part to uncertainties in the measured size distribution for particles 0.5 to 1.0 μm, and RH differences in the nephelometer (40%) and size distribution (20%) measurements, due to the hygroscopicity of the marine aerosol. Rood et al. [*1987*] show that there can be a 20% difference in the light scattering coefficient between these humidities.

The hygroscopic growth factor, $f_{RH}(\sigma_{sp})$, was estimated using the measured particle size distribution for various values of diameter growth factor, $f_{RH}(D_p)$. The results are shown in Fig. 3. The hygroscopic growth of aerosol scattering, $f_{85\%}(\sigma_{sp})$, if one assumes the same aerosol composition and a $f_{RH}(D_p)$ of 1.6,

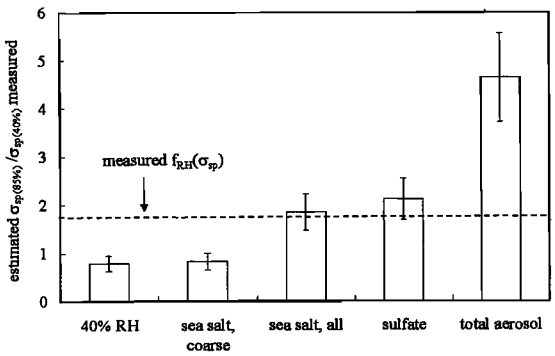

Figure 5. The increase in σ_{sp} due to hygroscopic growth of aerosol components at 85% RH. The uncertainty in the value at 40% RH is from a 20% change in the refractive index, while uncertainties in the reported values at 85% are from using diameter growth factors of 1.5 and 1.7, with a constant refractive index.

would be 2.8 for the marine case, and 6 for the anthropogenically influenced case, owing to the smaller particle size distribution of the anthropogenic case. In contrast, the measured $f_{85\%}(\sigma_{sp})$ is 2.7 for the marine case and 1.7 for the anthropogenic case. These results imply that aerosol composition, rather than differences in the particle size distribution, is responsible for the observed differences in $f_{RH}(\sigma_{sp})$.

The relative abundance of each aerosol type, determined from EM, was used to estimate its relative contribution to the aerosol light scattering as a function of size, as shown in Fig. 4. Not surprisingly, the aerosol composition (sub 1 μm) is predominantly sea salt for the marine case representing ~95% of σ_{sp} at 40% RH, with a small contribution from sulfate and mineral aerosol. For the anthropogenic case the aerosol composition was more varied, with sea salt contributing ~40% of the sub 1 μm scattering. Mineral, carbonaceous and sulfate aerosol were responsible for the remainder. Due to the difficulty in estimating the amount of organic carbon in internally mixed particles, our results suggest that it is at least as abundant as sulfate aerosol. The results also suggest that non-hygroscopic mineral and carbonaceous aerosol contributed to the observed differences in hygroscopic behavior. Indeed, if we assume a $f_{RH}(D_p)$ of 1.6 for sea salt aerosol and no appreciable growth for the remaining aerosol types in the anthropogenically influenced sample, the light scattering enhancement is 1.9 ± 0.4, sufficient to account for the measured hygroscopic growth (Fig. 5). This suggests that the only hygroscopic component for the anthropogenic case is sea salt aerosol and that other aerosol constituents do not grow appreciably; alternatively we suggest that the growth of sea salt aerosol is suppressed, allowing for a limited amount of growth associated with other aerosol types. This would imply internal mixtures of non-hygroscopic material associated with sea salt and sulfate particles.

Acknowledgments. The research was supported by a National Research Council Postdoctoral Fellowship and by an appointment to the Global Change Distinguished Postdoctoral Fellowship Program. We thank NCEM for access to the AEM, Teresa Miller at NOAA PMEL for technical assistance and Joyce Harris for trajectory analysis. NCEM is a US DOE facility at Lawrence Berkeley National Laboratory, which provides users with state-of-the-art instrumentation at no-charge after proposal review and approval. Work at Brookhaven National Laboratory was supported by the Environmental Sciences Division of the U. S. Department of Energy (DOE) as part of the Atmospheric Chemistry Program and was performed under the auspices of DOE under Contract No. DE-AC02-76CH00016.

References

Bergin, M. H., J. A. Ogren, S. E. Schwartz, and L. M. McInnes, Evaporation of ammonium nitrate aerosol in a heated nephelometer: Implications for field measurements, *Environ. Sci. and Techn.*, 31, 2878-2883, 1997.

Bohren, C. F., and D. R. Huffman, *Absorption and scattering of light by small particles*, Wiley and Sons, New York, 1983.

Charlson, R. J., S. E. Schwartz, J. M. Hales, R. D. Cess, J. A. Coakley, Jr., J. E. Hansen, and D. J. Hoffman, Climate forcing by anthropogenic aerosols, *Science*, 255, 423-430, 1992.

Covert, D. S., R. J. Charlson, and N. C. Ahlquist, A study of the relationship of chemical composition and humidity to light scattering by aerosols, *J. Appl. Met.*, 11, 968-976, 1972.

Harris, J. M., and J. D. W. Kahl, Analysis of 10-day isentropic flow patterns for Barrow, Alaska: 1985-1992, *J. Geophys. Res.*, 99, 25845-25855, 1994.

Hegg, D. A., D. S. Covert, M. J. Rood, and P. V. Hobbs, Measurements of aerosol optical properties in marine air, *J. Geophys. Res.*, 101, 12893-12903, 1996.

Hoppel, W. A., J. W. Fitzgerald, G. M. Frick, R. E. Larson, and E. J. Mack, Aerosol size distributions and optical properties found in the marine boundary layer over the Atlantic Ocean, *J. Geophys. Res.*, 95, 3659-3686, 1990.

Koloutsau-Vakakis, S., M. J. Rood, The $(NH_4)_2SO_4$-Na_2SO_4-Na_2SO_4-H_2O system: Comparison of deliquescence humidities measured in the field and estimated from laboratory measurements and thermodynamic modeling, *Tellus*, 46B, 1-15, 1994.

McInnes, L. M., D. S. Covert, B. M. Baker, The number of sea-salt, sulfate, and carbonaceous particles in the marine atmosphere: EM measurements consistent with the ambient size distribution, *Tellus*, 49B, 300-313, 1997.

McMurry, P. H., and M. R. Stolzenburg, On the sensitivity of particles size to relative humidity for Los Angeles aerosols, *Atmos. Environ.*, 23, 497-507, 1989.

Ogren, J. A., S. A. Anthony, J. Barnes, M. H. Bergin, W. Huang, L. M. McInnes, C. Myers, P. Sheridan, S. Thaxton, and J. Wendell, *Aerosols and Radiation*, NOAA Climate Monitoring and Diagnostics Laboratory Summary Report, 1994-1995, 1996.

Pueschel, R. F., R. J. Charlson, and N. C. Ahlquist, On the anomalous deliquescence of sea-spray aerosols, *J. Applied Met.*, 8, 995-998, 1969.

Rood, M. J., T. V. Larson, D. S. Covert, and N. C. Ahlquist, Measurement of laboratory and ambient aerosols with temperature and humidity controlled nephelometry, *Atmos. Environ.*, 19, 1181-1190, 1985.

Rood, M. J., D. S. Covert, and T. V. Larson, Hygroscopic properties of atmospheric aerosols in Riverside, California, *Tellus*, 39B, 383-397, 1987.

Schwartz, S. E., The whitehouse effect-Shortwave radiative forcing of climate by anthropogenic aerosols: An overview, *J. Aeros. Sci.*, 27, 359-382, 1996.

Svenningsson, I. B., H. C. Hansson, A. Wiedensohler, J. A. Ogren, K. J. Noone, and A. Hallberg, Hygroscopic growth of aerosol particles in the Po Valley, *Tellus*, 44B, 556-569, 1992.

(Received August 20, 1997: revised December 10, 1997; accepted December 19, 1997.)